Design of an Aerodynamic Lens for PM2.5 Chemical Composition Analysis

Dragan Nikolić[1],
California Institute of Technology, Jet Propulsion Laboratory, 4800 Oak Grove Drive, Pasadena, CA, 91109

David Keicher[2], and Fa-Gung Fan[3]
Integrated Deposition Solutions, Inc., 5901 Indian School Rd NE Suite 125, Albuquerque, NM 87110

The NanoJet aerodynamic lens by Integrated Deposition Solutions (IDS) differs from other designs in its use of sheath gas, which in turn enables us to achieve nearly 100% transmission efficiencies for particles in 1-6 μm size range. In this initial study we explore required operating conditions under which the Nanojet technology will efficiently concentrate aerosol particles suspended in the cabin air onboard the International Space Station (ISS). The Nanojet technology will serve as an aerosol sample inlet, concentrator, and transfer line to the Jet Propulsion Laboratory (JPL) quadrupole ion trap (QIT) mass spectrometer (MS) where real-time chemical analysis of aerosol composition will be performed. In the present study test particles are assumed to have a mass density of 2g/cm^3 representing metallic (aluminum) core with hydrocarbon envelope.

Nomenclature

IDS	=	Integrated Deposition Solutions	Al-Cl-Zr	=	aluminum zirconium tetrachlorohydrex
ISS	=	International Space Station	Fe-Cr-Ni	=	austenitic stainless steel
JPL	=	Jet Propulsion Laboratory	Fe-Cr-Al	=	Kanthal
QIT	=	Quadrupole Ion Trap	Al-Si-Fe	=	4006 aluminum alloy
MS	=	Mass Spectrometer	μm	=	micrometer
S.A.M.	=	Spacecraft Atmosphere Monitor	*Re*	=	Reynold number
sccm	=	standard cubic centimeter per minute	PM2.5	=	Fine particulate matter smaller than 2.5μm

I. Introduction

THE recent results[1] on the indoor air quality of the International Space Station (ISS) revealed that filtered particles (visible high-contrast metals greater than 1 μm) had an average diameter of 6.3 μm and either had complex morphologies or consisted of multiple metals embedded in a carbonaceous matrix. The most abundant metallic aerosols were aluminum zirconium tetrachlorohydrex (Al-Cl-Zr) alloy, austenitic stainless steel (Fe-Cr-Ni, 7.7 g/cm^3), Kanthal (Fe-Cr-Al, 7.1g/cm^3), and 4006 aluminum alloy (Al-Si-Fe, 2.7 g/cm^3). Real-time detection of single-component aluminum particles with sizes smaller than 2.5μm (PM2.5), salts, and hydrocarbon aerosols is of great importance for monitoring the quality of cabin air. However, to extract trace levels of aerosols from the dominant gas phase (cabin air) without exceeding the capacity of the differential pumping system, see Figure 1, requires optimization of the pressure gradient from the inlet orifice to the outlet nozzle and downstream to the mass spectrometer (QIT-MS) where the aerosol chemical composition analysis is performed.

Cabin air is sampled at the reduced flow rate through an orifice such that the pressure inside the relaxation tube does not exceed 30Torr, see Figure 1. Heavy aerosol particles tend to stay close to the flow axis whereas lighter molecules from the gas phase tend to diffuse away from the flow axis. If the inlet of the Nanojet flow cell is attached to the relaxation tube, and its outlet nozzle is kept at the lower pressure, it is expected that the established axial flow will contain aerosols and that the ligher gas phase will constitute the peripheral sheath flow. When exiting the outlet

[1] Technologist, 389T - Planetary Mass Spectrometry, Mail Stop: 306-392.
[2] Vice President, IDS Inc.
[3] Consultant, IDS Inc.

nozzle, gas phase molecules will diffuse off-axis and will be redirected by skimmers to a differentially pumped regions evacuated by miniature turbo-molecular pumps (mTMP). Because of their inertia, hevier aerosols will remain near the flow axis and after passing through skimmers will enter the QIT-MS vacuum chamber. This narrow beam of aerosols are vaporized on a hot filament and vapors are analyzed using electron impact ionization and mass spectrometry of generated ion fragments.

The pressure inside the QIT-MS vacuum chamber is maintained below 1E-6 Torr by combined action of miniature turbo-molecular (mTMP-3) pump and the ion/getter pump, see Figure 1. It is expected that vaporized aerosols are continuously chemisorbed by the getter pump and that any residual gas phase is removed via the mTMP-3 pump out of the vacuum chamber. Skimmed air in both differentially-pumped regions is continuously removed by mTMP-1 and mTMP-2 pumps, which are backed by the miniature scroll pump (mSP). Output from mSP can be filtered and recycled back into the relaxation tube as a sheath gas void of aerosols.

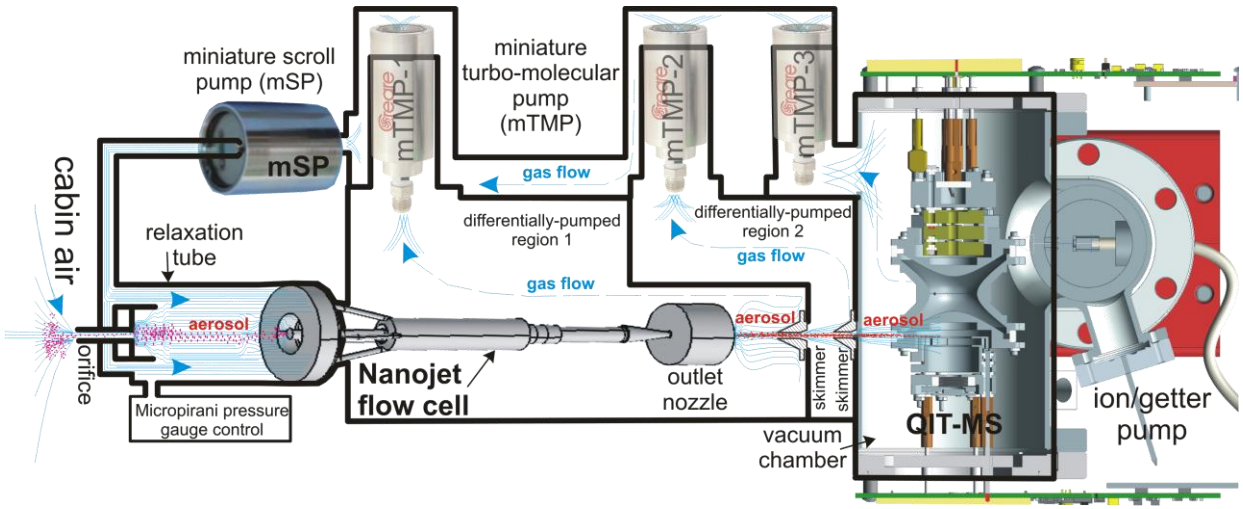

Figure 1: Aerosol mass spectrometer concept. Cabin air containing aerosol particles is sampled through an orifice and introduced into the Nanojet flow cell for aerosol focusing. The narrow particle beam coming out of the outlet nozzle is injected into the mass spectrometer (QIT-MS) where it is vaporized and analyzed. The Nanojet flow cell is 3" long and is part of technology patented by the Integrated Deposition Solutions (IDS) and will be used here as an efficient aerodynamic lens to focus aerosols into a narrow beam.

The main objective of the present study is to redesign the flow cell of the NanoJet printer head[2] by maximizing its transmission probability for hydrocarbon aerosols with metallic core as a function of their size and density. Airborne debris[1] collected onboard ISS had sizes from 10nm to several hundreds of micrometers. It consisted of synthetic fibers from clothing, fiberglass and titanium dioxide, and various combinations of 27 heavy metals embedded in carbonaceous matrix (70% by weight[1]). These particulates present health hazard in prolonged exposures and need to be continuously assessed as a part of ISS indoor air quality monitoring. Particles smaller than 10 μm in diameter may get trapped in the lungs and are likely to pass through the lungs into the bloodstream if smaller that 2.5 μm. Quantitative chemical analyses of particulates in the ISS cabin air require sample returns to Earth and use of standard laboratory equipment. It is thus advantageous to have a highly-efficient aerodynamic lens system as part of any mass spectrometer as it would enable quantitative real time chemical characterization of harmful aerosol pollutants.

By neglecting the gravitational settling at various flow rates, the goal is to determine aerosol transportation losses due to radial diffusion of particles while being carried into the deposition head nozzle, see Figure 2(a). These losses are expected to be minimal in the sheath gas design, which will prevent aerosol collisions with aerodynamic lens walls. The purpose of the sheath flow is to provide the particle-free gas layer between the aerodynamic lens walls and the particle laden stream carrier gas to avoid aerosol impactions onto the aerodynamic lens surface. As a result the addition of the sheath gas enables very high transmission efficiencies in the aerodynamic lens apparatus. At present, we report only the initial results on the optimal flow rates and system geometry that will reduce transport losses due to radial diffusion. We investigated aerosols 1-6 μm in size and density of 2 g/cm^3, which are representative for particulates containing aluminum core and hydrocarbon envelope. Design of new aerodynamic

lens and supporting differential pumping system are intended to be used as a future sample inlet for the Spacecraft Atmosphere Monitor (S.A.M.)[3,4], which will be modified to vaporize aerosols and analyze their chemical composition.

II. Methodology

The proprietary Nanojet flow cell design methodology is described in detail elsewhere[2] and will not be discussed here as it is thourougly tested in industrial applications. Instead we provide a general introduction into its engineering 3D model and summarize simulated performance. Aerodynamic flow focusing is well known and allows the trace level analytes to be axially confined by radially squeezing the analyte with the side streams of buffer (sheath) flow. Analyte is in our case aerosol particles suspended in an unfiltered cabin air and being continuously sampled and injected into the central aerosol tube as shown in Figure 2(a). The buffer (sheath) gas flow can be due to filtered air and at the exit nozzle the width of the central aerosol stream is a complex function of geometry, type, and relative rate of flow between analyte and sheath gas. In general, aerodynamic flow focusing requires that central analyte flow is parallel and confined between the currents of sheath flows. For this analysis flow-focusing is achieved when sheath flows meet the central aerosol flow at 60 degrees.

The Nanojet flow cell 3D geometry in Figure 2(a) is modeled using COMSOL Multi-Physics software (version 5.1). The main advantage of using COMSOL as a unified modelling platform[5] is the ability to deploy several physics phenomena into a single analysis. Modelling involved building a 3D representation of Nanojet flow cell geometry, selection of physics module, assigning initial values and defining boundaries, unstructured meshing, and particle tracing. Prior to the modelling of particle trajectories and computing transmission efficiencies, we compute the velocity field for air as a medium through which particles will propagate[6]. Low Reynold number values (Re < 2000) indicated presence of laminar flow conditions, thus the physical module chosen in COMSOL was laminar flow module coupled with particle tracing module. Meshing of 3D flow space geometry into smaller tetrahedral volumes as well as triangulation of boundary surfaces was done iteratively in order to balance the convergence of

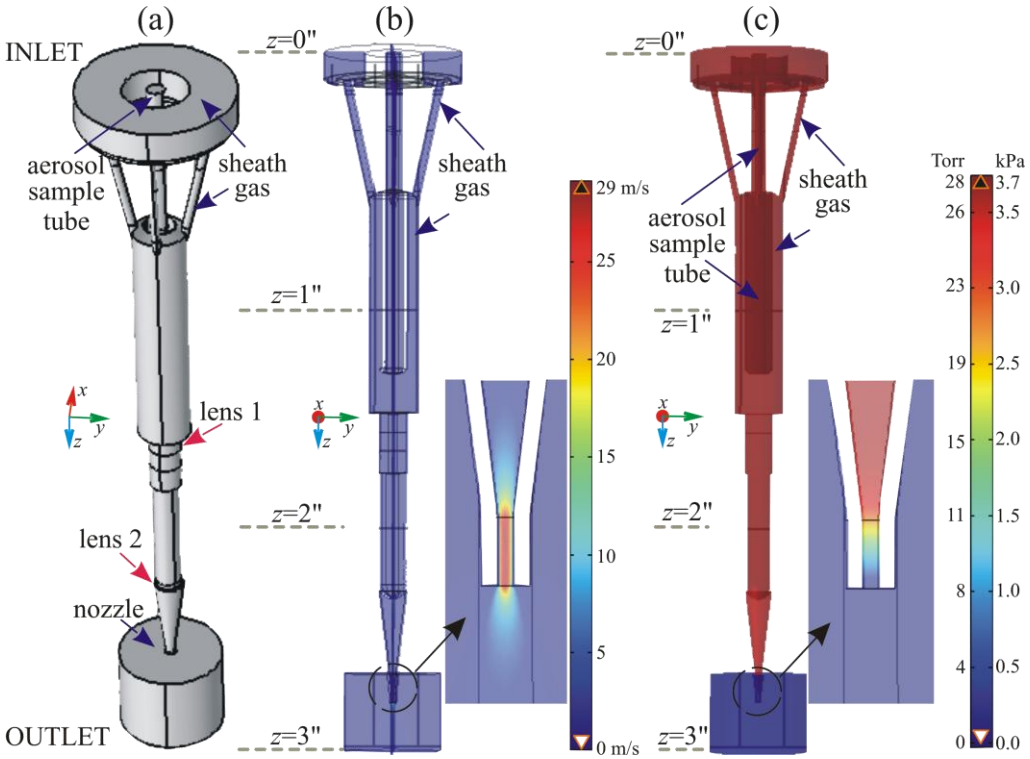

Figure 2: Nanojet gas flow field. (a) central tube serves for introduction of aerosol into the sheat gas flow, which carries aerosol particles through collimating lenses and beams aerosols out from the nozzle; (b) axial distribution of carrier gas velocity that supports high transmission of 1-6μm particles; (c) axial distribution of carrier gas pressure required for establishing and maintaining the indicated velocity field.

velocity distribution and required computational time. Adaptive unstructured meshing near the curved surfaces is used to represent flow volume such that sizes of finite elements never exceed 0.1% of the local curvature radius. Regarding the initial conditions, we specify inlet and outlet velocities in terms of the sheath gas and aerosol sample gas flow rates. The sheath and aerosol gas flow rates were set to 45 and 8 sccm, respectively. "No-slip" boundary condition ensures that the sheath gas comes to rest at the flow cell walls. The density of the aerosol particles was set to 2g/cm^3. Figure 2(b) summarizes composite velocity field due to both the sheath and the aerosol-free analyte flows and the maximum air supply velocity of the model can be determined using the provided color range bar. Color map contains the magnitude of the velocities in the YZ plane for five different sections of the Nanojet flow cell with velocity being greatest along the cell's Z-axis. Figure 2(c) provides the corresponding axi-symmetric pressure distribution, which is gradually decreasing from the gas inlets as we move along the flow cell towards the exit

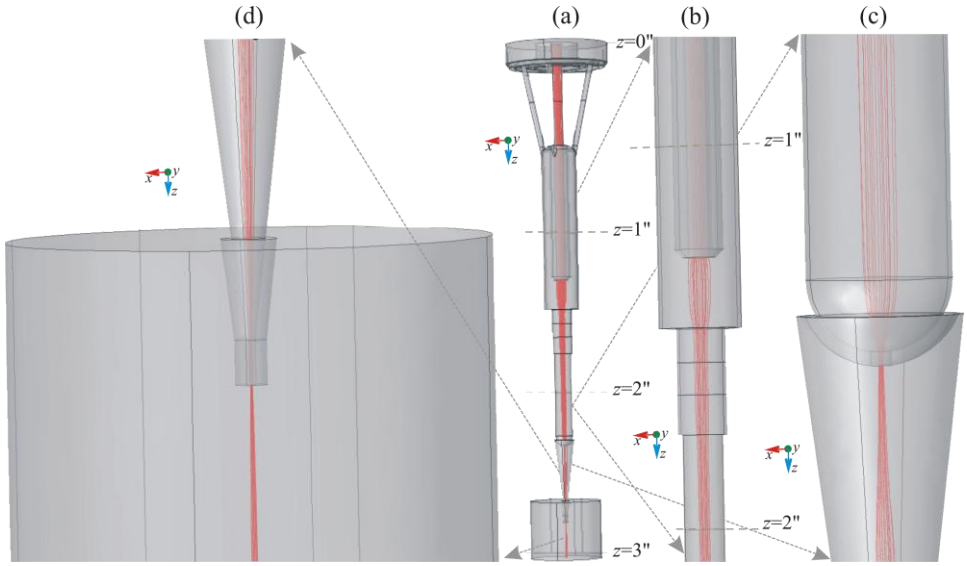

Figure 3: Drag-driven 1μm particle movement and tracing with mass. (a) Aerosol particles are initially uniformly released into the aerosole tube and their trajectories, here given as solid red curves, are traced along the whole length of the Nanojet flow cell. Enlarged sections of the flow cell corresponding to the first (b) and the second (c) aerodynamic lenses. (d) Focusing of aerosol trajectories into a particle beam at the exit nozzle.

nozzle. Previous experimental results[7] show very good Nanojet print quality for liquid aerosol droplets for 4 hour periods with no measurable decrease in aerosol beam width or flow resistance. At the same time monitored pressure drop through the Nanojet print head show variations only at the 3rd significant digit.

It is in this velocity/pressure field that we release aerosol particles uniformly across the inlet of the aerosol tube, and trace their trajectories until they reach the exit nozzle or collide with cell walls (see Figures 3(d) and 4(c) for trajectory details). In finding the optimal flow rates for the given particle size and density, we minimize the number of trajectories that collide with cell walls and maximize the number of trajectories that are focused in a beam at the exit nozzle. In our simulations, the minimum width of the particle beam was observed when the ratio of the sheath flow to the sample flow was 5.6.

III. Results and Discussion

We will present only the final results with respect to the particle tracing as the function of their size. Systematic search for optimal flow rates and final simulation settings will not be reported here. Figure 3 illustrates trajectories of 1μm aerosol particles as they undergo drag-driven motion through different sections of the Nanojet flow cell. The volume occupied by both the sheath gas and the sample gas is given in gray color whereas trajectories of aerosol particles as they undergo squeezing along Z-axis are given in red color. The cross-section view (YZ-plane in Figure 3(a)) of particle trajectories shows how inititally uniform distribution of aerosol particles at the inlet of the aerosol tube embedded into the central sample gas flow becomes radially compressed as flow progress toward the exit nozzle.

Inset in Figure 3(b) provides a view of trajectories for 1μm aerosol particles as they travel through and exit from the central aerosol tube, after which they mix with the sheath flow and get transferred into the first aerodynamic

lens. Trajectories are near-parallel after they exit the first lens and enter the second lens shown in Figure 3(c). Finally, particles are further focused at the exit nozzle as shown in Figure 3(d). The width of the aerosol beam at the exit nozzle is estimated to be between 20-40μm. We note that the smaller aerosol beam widths at the exit nozzle are expected for larger particles. This effect is illustrated in Figure 4 for 6μm aerosol particles. It is expected that changes in the aerodynamic lens set would improve focusing of all particle sizes.

In Figure 4(a) we show an enlarged section of the Nanojet flow cell featuring traces of particle motion through both the first and the second aerodynamic lenses. We further enlarge in Figure 4(b) the lower part of this section to show the second lens only, and how it affects the focusing of the aerosol beam. It is evident from Figure 4(c) that due to the larger motional inertia, the beam for 6μm aerosol particles is narrower compared to the case of 1μm particles traces shown in Figure 3(d).

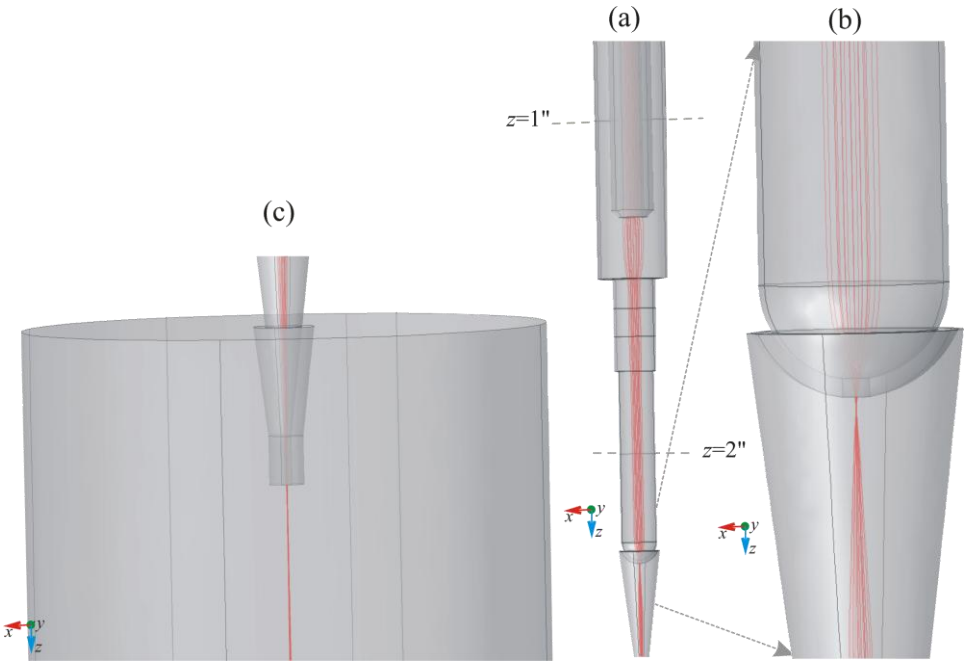

Figure 4: Drag-driven 6μm particle movement and tracing with mass. Refer to Figure 3 for details. The enlarged sections of the Nanojet flow cell are as follows: (a) the fist aerodynamic lens, (b) the second aerodynamic lens, and (c) the exit nozzle with focused aerosol beam trajectories.

IV. Conclusion

We have presented a simulation study in which we identified optimal flow rates for both the buffer (sheath) gas and the sample gas containing aerosols. Buffer gas is assumed to be aerosol-free, but in future studies we will explore the effects of including the particulate phase into the sheath flow as well. Obtained results suggest that the aerosol particles can be focused into a narrow beam and as such transferred into a differentially pumped module for further removal of the gas phase. The lighter gas phase will undergo faster radial thermal expansion than heavier aerosols when subsequently transferred from high to low pressure segments of the differentially pumped module. As a result, the heavier aerosol beam is expected to retain its low divergence and remain confined axially. Effectivelly, the differential pumping module will act as aerosol particle filter as it separates ligher gas phase from the heavier particulate phase. This relative enrichment of aerosols with respect to gas phase will improve sensitivity of the JPL QIT-MS to sub ppb levels, and ensure that ion/getter pumps do not saturate due to dominant gas phase entering the mass spectrometer.

Acknowledgments

This work has been partially carried out at the Jet Propulsion Laboratory, California Institute of Technology, under the contract with the National Aeronautic and Space Administration. © 2019. California Institute of Technology. Government sponsorship acknowledged.

References

[1]M.E. Meyer, *Results of the Aerosol Sampling Experiment on the International Space Station*, 48th International Conference on Environmental Systems, 8-12 July 2018, Albuquerque, New Mexico; article ICES-2018-100.

[2] M. Essien, *Apparatuses and Methods for Stable Aerosol Deposition Using an Aerodynamic Lens System*, US Appl. 14/927380 (2016).

[3] S. M. Madzunkov, S. Schowalter, D. Nikolic *et al.*, *Progress Report on the Spacecraft Atmosphere Monitor's Development Model*, 48th International Conference on Environmental Systems, 8-12 July 2018, Albuquerque, New Mexico; article ICES-2018-325.

[4] S. Schowalter, S. M. Madzunkov, M. Darrach *et al.*, *The Technology Demonstration of the Spacecraft Atmosphere Monitor*, 49th International Conference on Environmental Systems, 7-11 July 2019, Boston, Massachusetts; article ICES-2019-321.

[5] R. W. Pryor, Multiphysics Modeling Using COMSOL: A First Principles Approach, Sudbury, Massachusetts: Jones and Bartlett (2011).

[6] D. W. Pepper D. Carrington, Modeling Indoor Air Pollution, London, UK: Imperial College Press (2009).

[7] D. Keicher and M. Essien, *Advancing Aerosol Printing for Fine Features and Gradient Structures*, NextFlex Workshop: FHE Applications for Aerospace, April 1–4, 2019, Seattle, Washington; lecture in Session III: Conformal/Flexible Electronics and Antennas for Aircraft (2019).